

Assembly and dynamics of propelling ferromagnetic colloids

Author: Andrés Javier Manzano González

Facultat de Física, Universitat de Barcelona, Diagonal 645, 08028 Barcelona, Spain.

Supervisors: Gaspard Junot & Pietro Tierno

(Dated: June 2023)

Active colloids is a growing field of research that studies the emergent phenomena exhibited in systems of self-propelling particles as a result of the interactions between them that could not be observed if these components were isolated. These phenomena can be observed in a wide variety of systems. In this work, I show how a collection of oscillating colloidal rotors, or simply, shakers, immersed in a viscoelastic fluid, specifically, a solution of polyacrylamide (PAAM), can display this behaviour, forming complex zig-zag dynamic bands that grow linearly in time. I have investigated the dynamics of this band growth for two different PAAM concentrations, as well as the hydrodynamic flow around these shakers for both cases. This helps understanding the complex dynamics of these fluids, having implications in soft matter physics and microfluidics and in biophysics.

I. INTRODUCTION

This work has been done within the context of soft matter physics. Soft matter physics is a research area that focuses on the study of systems in which interactions between the components are of the same order of magnitude as thermal energy, $k_b T$. This means that the dynamics occurring in soft matter systems, such as the internal molecular rearrangement, can be considered slow, and such systems have easily accessible length and time scales. This work concentrates specifically on viscoelastic fluids, which are materials that behave as elastic solids at short time scales and flow as liquids at long time scales, thus displaying both elastic and viscous properties under external deformations.

Active [1–4] and externally-propelled microscopic particles [5–7] moving in viscoelastic fluids constitute a growing field of research, in which many emergent non-equilibrium phenomena can be observed [8]. Due to their accessible length and time scales, colloidal suspensions constitute an appropriate means to observe these emergent phenomena [9, 10]. Colloids are small particles that may be considered as large atoms, as they are small enough to display thermal fluctuations similar to atoms, but large enough that the dispersing medium can be considered as a continuum. Also, colloidal particles display micrometric size and their range of speed of the order of $\mu m s^{-1}$, thus, similar to that of many the microorganisms we want to mimic; for these reasons, they represent a suitable model system for biological media. Moreover, given their size, speed and the viscosity of the dispersing medium, we can neglect the inertial force, meaning we are working at low Reynolds number. In this TFM project, using magnetic colloids, I will show that a collection of active shakers driven by an external rotating magnetic field can self-organise into large-scale dynamic chains that exhibit a zig-zag configuration, as well as the microscopic flow around them.

II. THEORETICAL BACKGROUND

A. Soft matter and viscoelastic fluids

Matter can respond to external stresses in various complex manners. The two extreme behaviors are known as "elastic solid" and "viscous fluid" ones. The ideal elastic solid, when submitted to a shear strain, σ will suffer a proportional shear strain, as can be seen in Fig. 1. These solids follow a kind of Hooke's law, $\sigma = G\gamma$, where

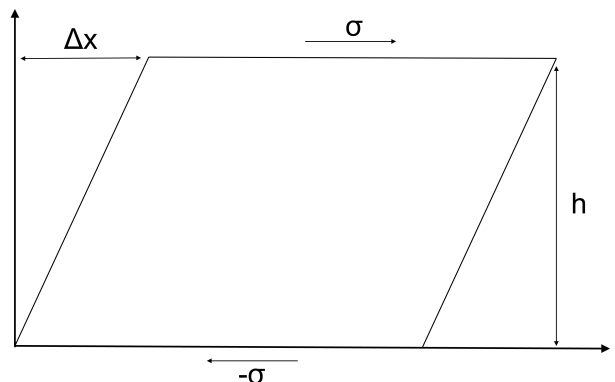


FIG. 1: Shear stress and strain in an ideal elastic solid. Here, h is the elevation of the solid and Δx the displacement induced by the applied stress

G is the elastic modulus, similar to the spring constant k , and $\gamma = \frac{\Delta x}{h}$. Note that, when the stress stops, it goes back to its original shape. Instead, when an ideal viscous fluid is submitted to a shear stress, it flows, the material does not maintain its shape, and its shear rate is given by $\dot{\gamma} = \frac{\sigma}{\eta}$, with $\dot{\gamma} = \frac{\partial \Delta x}{\partial t} \frac{1}{h}$, with the dot representing the derivative with respect to the time, with η being the dynamic viscosity, which defines how easily the fluid flows when subjected to body forces. Fluids that display a constant viscosity for any applied stress are called "Newtonian fluids".

In contrast to Newtonian fluids, elastic solids have an infinite memory of their shape, and no matter how much time I deform them, they will always go back to the original configuration, whereas viscous fluids have no memory, and will immediately forget their previous structure and instantly adapt to the new one. If I were to put in terms of energy, the elastic solid stores all the elastic energy of the stress applied to them, while the viscous fluid dissipates it.

A viscoelastic fluid, as its own name suggests, is a material that displays both elastic solid and viscous fluid properties, depending on the time scale, i.e., depending on the duration. At short time scales, the fluid is able to store some elastic energy of deformation, "remembering" its original form; however, as the deformation continues, it starts to dissipate this energy, and "forgetting" how it originally was, thus, flowing. When submitted to an oscillatory shear stress, for small frequencies, meaning long time scales, the viscoelastic fluid will behave as a liquid, dissipating all the energy, whereas for greater frequencies, it will act more like a solid, storing a large part of it. The stress response of a viscoelastic fluid to an oscillatory shear stress for small strains is given by Eq. 1.

$$\sigma(t) = \gamma_0[G'(\omega)\sin(\omega t) + G''(\omega)\cos(\omega t)] \quad (1)$$

With γ_0 being the amplitude of the strain ($\gamma_0 \ll 1$), $G'(\omega)$ and $G''(\omega)$ complex moduli which represent, respectively, the energy stored by the material and the energy dissipated in the system. In Fig. 2, we can observe the value of these moduli as a function of the frequency ω for a viscoelastic fluid, namely, an aqueous solution of 0.5% polyacrylamide (PAAM). For small frequencies, the fluid stores more energy than what it dissipates, and, at around 2 rad/s, the situation changes.

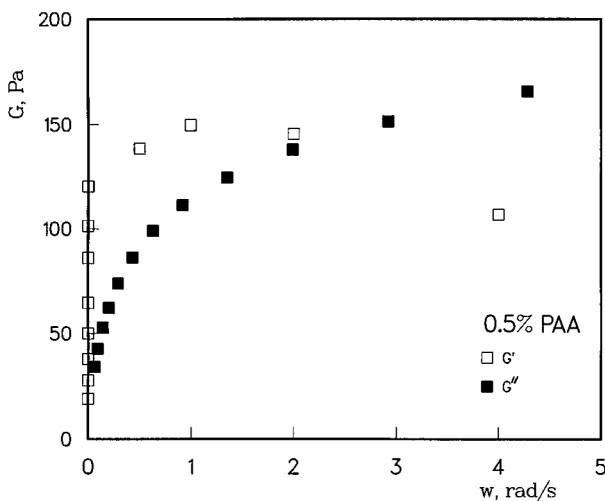


FIG. 2: Complex moduli $G'(\omega)$ and $G''(\omega)$ for an aqueous solution of 0.5% polyacrylamide (PAAM) [11].

Maxwell modelled these fluids in a very simple and intu-

itive way: as a spring connected with a viscous damper in series, with the strain of the system given by Eq. 2.

$$\dot{\gamma} = \frac{\sigma}{\eta} + \frac{\dot{\sigma}}{G} \quad (2)$$

. This model gives rise to a characteristic parameter: the relaxation time, $\tau_0 = \frac{\eta}{G}$, which is the time during which the material can store the elastic energy and "remember" its original configuration. According to Maxwell, all fluids are viscoelastic at sufficiently short time scales.

These phenomena, as we can see in Fig. 2, happen at accessible time scales; soft matter deals with this kind of materials, that display behaviors in between solids and liquids, such as viscoelastic fluids, gels, etc.

B. Colloids

Colloids are essentially, as previously explained, large atoms, from a thermodynamic point of view, since, at equilibrium, they can have the same equation of state as a classical ideal atomic gas [12]. They are large enough to be seen using optical techniques, and not to need quantum treatment, but small enough to experience random motion caused by the collision with the solvent molecules (Brownian motion), so, they have accessible lengths and time scales. They can also be used in passive microrheology, as we can relate their random movement in a fluid to the complex viscoelastic moduli of that fluid [13]. All this makes colloids suitable candidates to study a variety of phenomena in condensed and soft matter physics.

One can characterize the dynamics in colloidal system by measuring the Mean square Displacement (MSD) from the particle trajectories. The MSD is a parameter that characterises the random motion of small particle, since, naturally, the mean displacement of some random motion is zero, whereas its MSD differs from zero. As we see, for large values of time, it is linear with time, and one can extract the diffusion coefficient D . D relates the thermal energy to the viscous friction, and is an estimate of the average area covered by a particle per unit time during its random movement, indeed, it has units of $\mu m^2/s$.

C. The Navier-Stokes equation and the Reynolds number

The Navier-Stokes equations describe the dynamics of fluid systems. The most general way to express them is the following:

$$\frac{\partial \vec{v}}{\partial t} + (\vec{v} \cdot \nabla) \vec{v} = -\frac{1}{\rho} \nabla P + \frac{\eta}{\rho} \nabla^2 \vec{v} + \vec{f} \quad (3)$$

With ρ the density of the fluid, P the pressure, f an external force per unit volume, such as gravity. $\frac{\eta}{\rho}$ is known

as the kinematic viscosity. $(\vec{v} \cdot \nabla)\vec{v}$ represents the convective term, which describes the effect that the bulk motion of the fluid has on its own velocity. This term accounts for phenomena such as stretching, twisting, and shearing of fluid elements due to the velocity gradients in the flow; essentially, it represents the transfer of momentum within the fluid due to its own motion. The term $\eta \nabla^2 \vec{v}$ is the diffusive term, which accounts for the dissipation of momentum due to viscosity. These equations are very difficult to be solved analytically, since they require an hypothesis on the medium such as a constitutive relationship. In our particular case, our dispersing medium will be a non-Newtonian, incompressible fluid:

Firstly, let us examine the relation $\frac{(\vec{v} \cdot \nabla)\vec{v}}{\eta \nabla^2 \vec{v}}$. The term in the numerator is the convective term, which represents the inertial forces in my system, whereas, the term in the denominator, represents the dissipative forces, which that oppose this motion. Let V_0 be a typical value of $|\vec{v}|$, and L a typical length scale on which \vec{v} is varying, then we can define what is known as *Reynolds number*, R_e , given by:

$$\frac{|\rho \vec{v} \cdot \nabla \vec{v}|}{|\eta \nabla^2 \vec{v}|} \approx \frac{\rho V_0^2 / L}{\eta V_0 / L^2} = \frac{\rho V_0 L}{\eta} = R_e \quad (4)$$

In our case, colloids are very small objects ($L \ll 1 \text{ m}$), and the velocities reached in our case are small, thus, rendering the Reynolds number low ($R_e \ll 1$), thus, we can neglect the convective term, and we are left with:

$$-\nabla P + \eta \nabla^2 \vec{v} = 0 \quad (5)$$

Which is known as the Stokes equation. This equation is linear and independent of time, meaning it has time-reversibility, hence, reciprocal motion does not lead to propulsion [15].

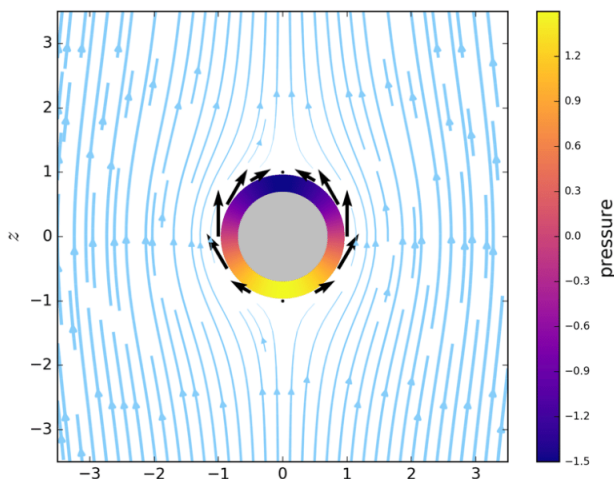


FIG. 3: Stokes flow around a sphere [14].

D.

III. EXPERIMENTAL SETUP AND METHOD

Our viscoelastic fluid is a solution of polyacrylamide (PAAM) in deionised water. The colloids used in the experiments are "peanut"-shaped hematite microparticles ($\gamma - Fe_2O_3$), as shown in Fig. 4. The synthesis process is explained in more detail in a previous work [9]. Essentially, a sodium hydroxide ($NaOH$) solution is slowly added to an iron chloride hexahydrate ($FeCl_3 - 6H_2O$) solution and stir it at $75 \text{ }^\circ C$ for 5 minutes; afterwards, another solution of potassium sulfate (K_2SO_4) is added to the mixture, and further stir it for 5 more minutes. Then, the mixture is hermetically sealed and let rest in an oven at $100 \text{ }^\circ C$ for 8 days. Finally, the solution is diluted with deionised water, and let the particles sediment; after removing the supernatant, the colloidal suspension is ready.

The self-organization of the magnetic colloids in the viscoelastic fluid is triggered by oscillating the particles back and forth. This motion is obtained by driving the colloids with an external magnetic field; since they have a magnetic dipole perpendicular to its long axis, see Fig. 8. The permanent magnetic dipole presented by the colloid has a value of $m \approx 9 \cdot 10^{-16} \text{ Am}^2$. An applied rotating magnetic field with a low frequency (such that permanent moment follow synchronously the field variation), it will induce a magnetic torque $\vec{T}_m = \vec{m} \times \vec{B}$, and so the colloid will rotate around its long axis. If the colloid was far away from any surface and in the bulk of a homogeneous medium, nothing would happen, as the rotational motion is reciprocal. However, since it is resting over a flat surface, the spatial symmetry is broken, originating net motion: colloids roll close to the surface due to the rotation-translation hydrodynamic coupling [16].

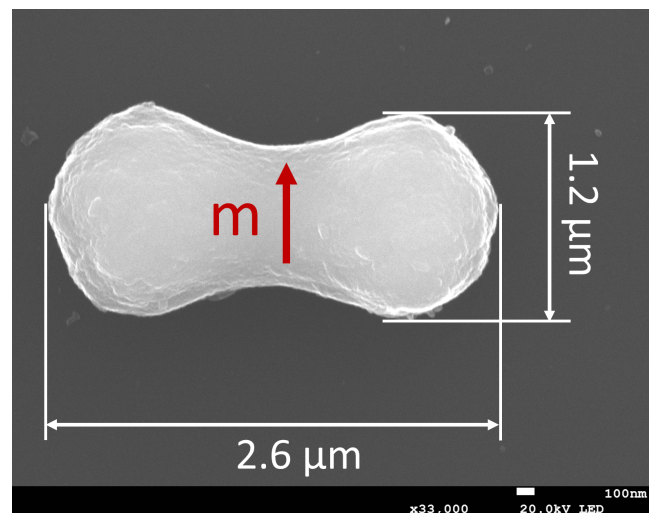


FIG. 4: Scanning electron microscope image showing one peanut shape colloid with superimposed in red the permanent magnetic moment.

To obtain an approximately constant magnetic field in our sample, we will use three coils: two perpendicular to the working plane and parallel to each other, responsible for the magnetic field along the y axis, and a third one parallel to the working plane, responsible for the magnetic field in the z axis. A representation of the top view of this setup can be seen in Fig. 5. The center of sample is placed at the center of the coil parallel to the working plane, at the point where these three axis converge. The camera is placed in the axis of the coil parallel to the ground. The magnetic field is produced using a wave generator, that induces an alternate current through the coils. If we use both coils to generate alternate magnetic fields with the same frequency and a phase difference of $\frac{\pi}{2}$, we can originate a circularly polarized magnetic field. Nevertheless, we want to make the particles move back and forth with zero mean displacement, i.e., we want to have them act as active shakers, so we need to change its direction periodically. To achieve this, we introduce a difference in the frequency of the fields generated by the coils, so the magnetic field in my sample is given by Eq. 6.

$$\vec{B} = B[\sin(2\pi t f_+) \hat{y} + \cos(2\pi t f_-) \hat{z}] \quad (6)$$

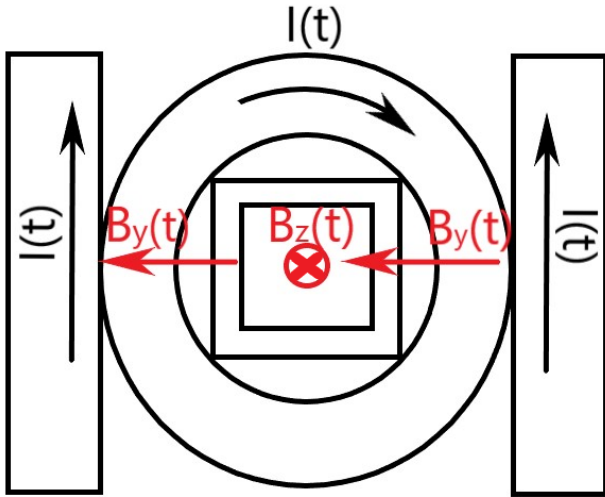
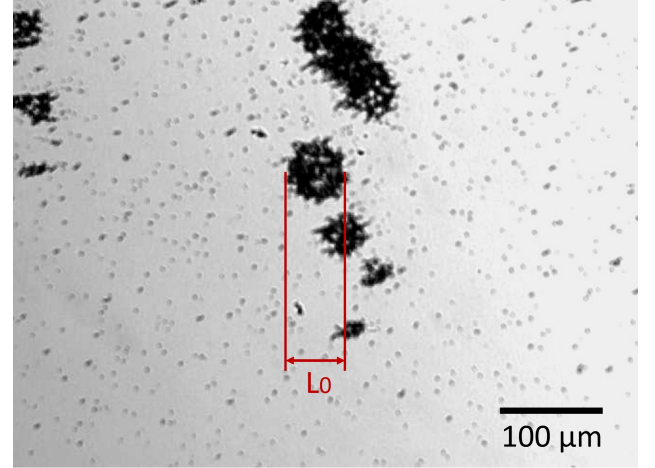


FIG. 5: Representation of the top view of the coils that generate a circularly polarised magnetic field.

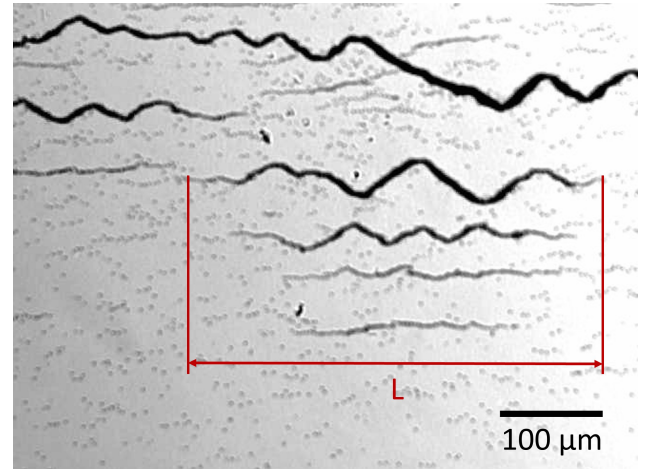
With $f_+ = f_0 + \frac{\Delta f}{2}$, $f_- = f_0 - \frac{\Delta f}{2}$ and $f_+ - f_- = \Delta f$. This will lead to a magnetic field that periodically switches its circular rotation. In our case, $f_0 = 80$ Hz, $\Delta f = 4$ Hz, and the amplitude $B = 5.5$ mT. This causes the colloids to move at an angular speed of $\Omega = 2\pi f_0$, since we are in the synchronous regime, and to switch directions periodically every $\Delta t = \frac{1}{2\Delta f}$, oscillating with an amplitude that depends on the concentration of PAAM, but typically of the order of $\Delta x \approx 0.5$ μm . We choose this frequency due to the fact that we need to move at a faster rate than the relaxation

time of the fluid, which, for a PAAM solution at these concentrations, is of the order of few milliseconds, $\tau \approx 3$ ms.

Since inertia is negligible, the Navier-Stokes equation should be time reversible for a Newtonian fluid, thus resulting in no net displacement. However, we are working with a viscoelastic one, i.e., non-Newtonian, so here the time reversibility is broken, and the colloids self-organise forming complex dynamic bands that grow over time, exhibiting a zig-zag configuration, as can be seen in Fig. 6.



(a)



(b)

FIG. 6: Several islands of colloids with an initial length L_0 (a) that grow over time to display complex chains (b) with length L .

The image in Fig. 6 was taken using a 10x lens, which is the one we will be using in this part of the experiment.

A. Method employed

The method used was the following: First, we need to prepare the PAAM solution, in order to do this, we weight the PAAM and the deionised water to ensure we have the desired concentration; then we add the PAAM to the water and stir it using a magnetic stirrer for 24 hours, to guarantee all the PAAM dissolves. Secondly, we need to make the colloids ready; they are stored in deionised water in the refrigerator; the reason they are stored at low temperatures is to reduce collisions between each other, which may result in aggregates due to the attractive Van der Waals interactions, accelerating their precipitation to the bottom of the container. After taking them from the refrigerator, we remove the supernatant, fill the container with deionised water and sonicate them, to separate the aggregates that may have formed while stored. We then add a surfactant to this dispersion, specifically, sodium dodecyl sulfate (SDS), which adheres to the surface of the colloids and prevents the formation of aggregates, and stir it until it is dissolved; lastly, once the SDS has dissolved we take a sample and sonicate it once again, to separate the aggregates, and, with this, we have the colloidal suspension ready. Finally, we mix the suspension with the PAAM in the right proportions to obtain the desired concentration, and put it in the rotator for one hour. After that, we have the sample ready to deposit on a slide and cover it using a cover slip, to observe it under the microscope and do the measurements.

The objective is to find colloidal aggregations that are semi isolated, i.e., that do not have any other colloids on the lateral sides, since those are the directions in which they will be growing. It is not relevant whether there are colloids above or below the initial cluster, since, as they will not grow along these directions. Thus, when preparing the sample, we first place a couple of drops of the colloidal suspension with PAAM previously prepared in the middle of the slide and some drops of the sole PAAM solution around it before covering it with the cover slip so that we have a region in the middle with colloids and a free region surrounding it. After that, we activate the magnetic field and let the bands grow outside of this region and into the colloid-free region. The result is a growing vertical line of colloids in the middle of a region in which there are no other particles. Now, in order to make smaller "islands" of colloids from this continuous line, I apply a rotating magnetic field in the xy plane (the working surface plane), as can be seen in the work done by Pietro, T. et al. [17]. By applying this magnetic field, the colloids will self-assemble into clusters, as shown in Fig. 6a, which then we can use as our initial clusters to grow the bands.

For the analysis of the videos, I used the commercial software Matlab. To extract the length of the chain, since the software is programmed in such a way to detect white objects, we have to invert the color of the video, so we have white colloids on a dark grey

background. Afterwards, we binarise the image, so we have a completely black background and colloids appear white, and detect the largest object on the frame. After that, we draw a bounding box surrounding it, and extract the length of the horizontal side of this box. We do this frame by frame, obtaining, effectively, the length of the chain in pixels per frame. We then need to convert pixels to μm and frames to seconds. In Fig. 7 we can see how the program detects the object and draws a bounding box around it. If there were many clusters,

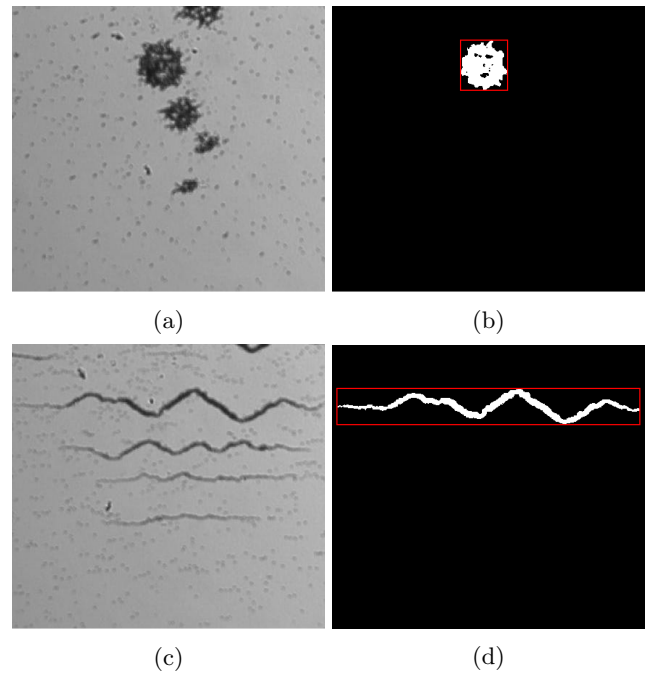


FIG. 7: Colloid cluster and chain detection.

we would first need to slice the video to choose the only cluster of interest leaving all the other aggregations out. In the next steps, I have to extract the microscopic flow around the colloids. This was achieved by using non-magnetic particles, so that they only interact with the hydrodynamic field, and track their position and velocities. For this purpose, we will use Silica colloids of a diameter of approximately $1 \mu m$ as tracers. This sample was prepared using a more diluted colloidal dispersion than previously, since we need to find isolated magnetic particles in our sample, and this will be easier in a more diluted dispersion. Additionally, we need to inject the right amount of tracers, neither too few so that I can get good measurements nor too many that they overlap, becoming unable to move freely and to properly follow the flow lines. For these measurements, I will use a 100x immersion oil lens. The sample seen through this lens can be observed in Fig. 8. To obtain the flow, we activate the magnetic field and start recording, since movements here are faster, we will need a higher frame rate than previously. Once the video is obtained, we track the position and velocity of every tracer at

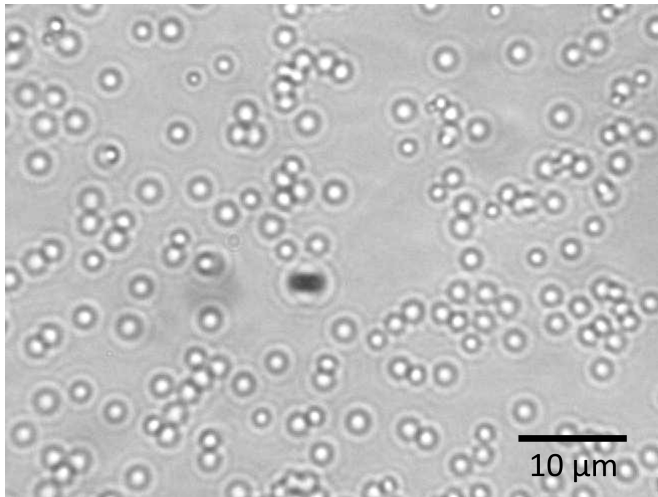


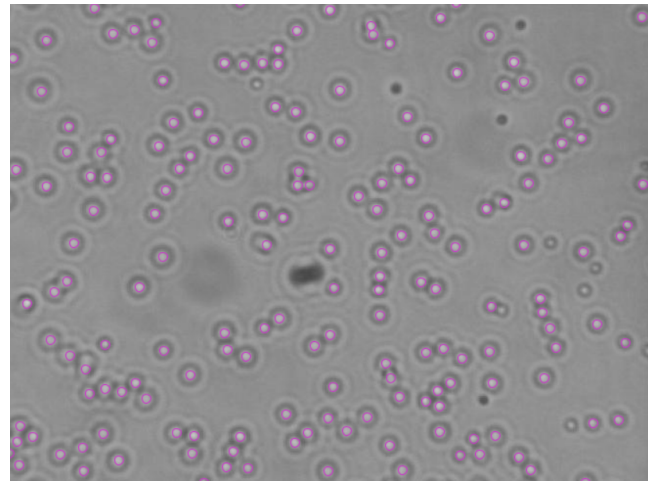
FIG. 8: Image of the sample seen through a 100x lens. The black particle is the magnetic colloid, the white particles are the tracers.

every frame, as well as the position of the magnetic colloid, and save these positions using ImageJ. This particle tracking can be seen in Fig. 9. As shown in this image, the silica colloids that can be considered to be far from the shaker move randomly mainly due to Brownian motion, whereas the ones close to it have a certain bias, as they move dragged by the hydrodynamic flow generated by the shaker. The objective is to find an isolated shaker, since the presence of more shakers in the proximity will alter the measured flow. To track the magnetic colloid, the procedure is the same, but we need to invert the color of the image, since the software can only detect white objects.

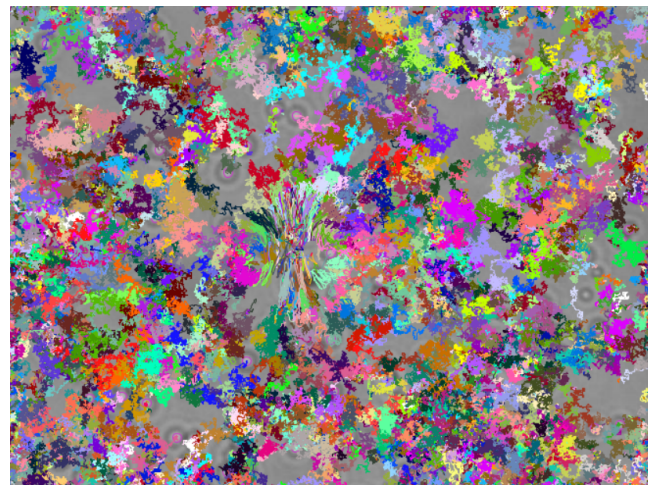
After obtaining a set of data with the frame number, position and velocity of each labeled particle, we proceed to use matlab for the rest of the analysis: we subtract the position of the peanut to the position of all of the tracers, so that it is set as the origin. Furthermore, I divide the screen into 4000 equal square cells, 200 divisions per side, and track the average vertical and horizontal velocity of all the tracers present on each cell at each frame. Once we have done this, we do a moving average over the neighbouring cells, to get smoother flow lines, to reduce fluctuations and noise in the signal, and, finally, due to the symmetry on the x and y axis, we can average the four quadrants to have better statistics.

IV. RESULTS AND DISCUSSION

We measured the flow and the growth rate of the bands for two different PAAM concentrations, 0.02% and 0.005%, to observe the influence of the medium in the behavior of the particles.



(a)



(b)

FIG. 9: (a) Tracers detected by the software ImageJ and (b) the path followed by each tracked tracer.

A. Growth rate

1. 0.02% PAAM

The pace at which the colloid aggregation grows depends, among other factors, on the number of colloids present in the aggregation, so, in order to compare the different measurements, the length of the chain L converted into the dimensionless variable, $\frac{L}{L_0}$, with L_0 being the initial horizontal length of the aggregation. We can see the growth rate of the chain in a solution of 0.02% PAAM in Fig. 10.

As we can see, there is some dispersion around the mean value of the different realisations of the experiment. This difference might be induced by several factors: firstly, the colloid clusters observed were not completely isolated, as there were some other particles around that may have affected the growing speed of the

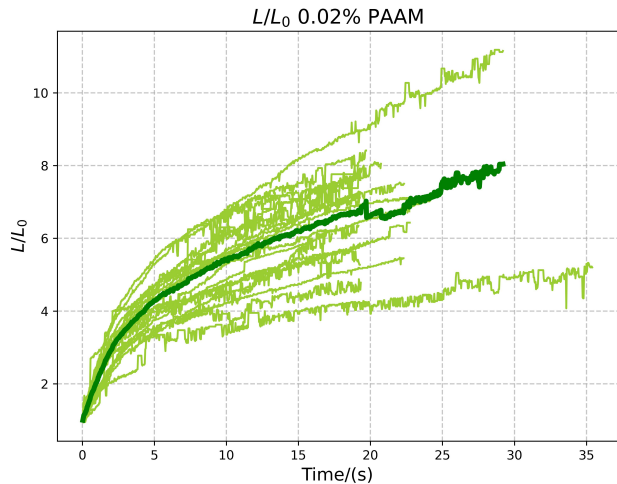


FIG. 10: Growth rate of the complex band for a concentration of 0.02% PAAM. In light green, the value of each experiment; in dark green, the mean value of all of them.

chain. On the other hand, the way we generated a rotating magnetic field that periodically changes directions can also play a role in this dispersion, since there is a net component on one direction, which might alter the results. Also, we have divided the length of the chain by its initial value, to obtain a dimensionless parameter, however, the speed at which it grows is not proportional to this initial length, but to the number of particles initially present in my cluster, however, this value is impossible to determine, since, due to the large density of particles in the initial cluster, they may be overlapping. Additionally, thermal fluctuations are non-negligible at this scale. Finally, the presence of impurities in my sample, such as dust or air bubbles, may also affect the measurements. In Fig. 11, the same figure can be observed in log-log scale.

In this figure, one can observe a clearer trend. The relation between the chain length and the time appears to be a power law, of the form $\frac{L}{L_0} \propto t^\beta$; nonetheless, we must take two considerations into account: there is a region at the beginning, up to around half a second, where the growth is slower. Although it may disturb the overall trend of data, one has to consider the lack of statistics: there are around 10 points in each trial, which is not enough to establish a proper relation. For larger values of time, the trend seems to be clearer, as it does resemble a power law, however, this region only spans one order of magnitude, in order to affirm the relation between the length of the bands and the time, longer measurements must be done; in spite of that, for this time window, the relation can be well fitted by a power law.

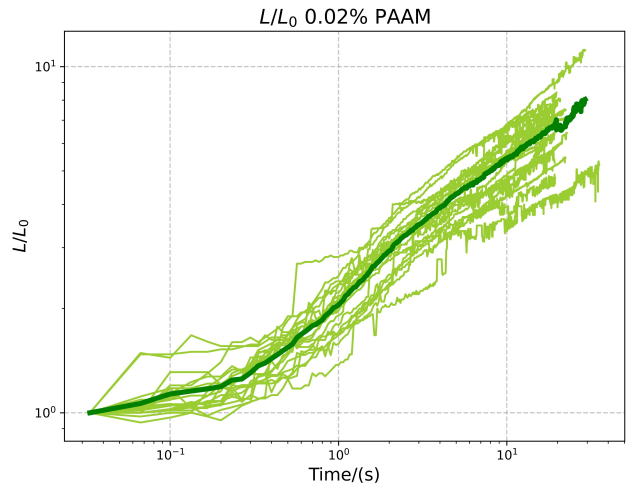


FIG. 11: Growth rate of the complex band for a concentration of 0.02% PAAM in log-log. In light green, the value of each trial; in dark green, the mean value of all the trials.

2. 0.005% PAAM

Now, let us do the same analysis for the 0.005% PAAM solution. In Fig. 12, the dimensionless variable $\frac{L}{L_0}$ as a function of time can be seen.

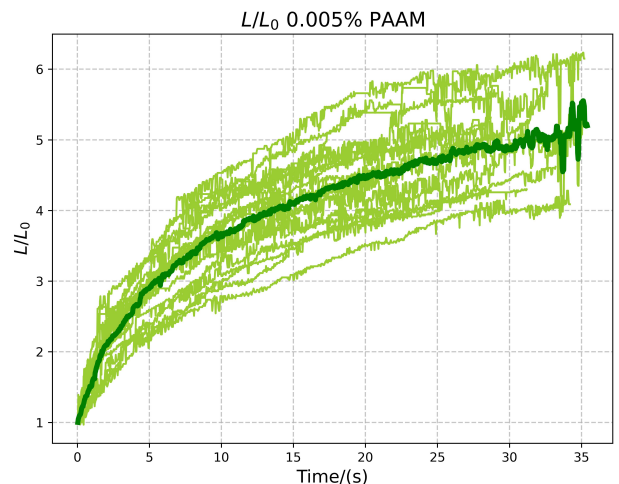


FIG. 12: Growth rate of the complex band for a concentration of 0.005% PAAM. In light green, the value of each experiment; in dark green, the mean value of all of them.

As can be seen, we get similar results as previously, although this time, the dispersion of the measurements is smaller, and the growth pace is visibly slower. To observe a clear trend, just like before, the same plot but

in log-log scale can be seen in Fig. 13.

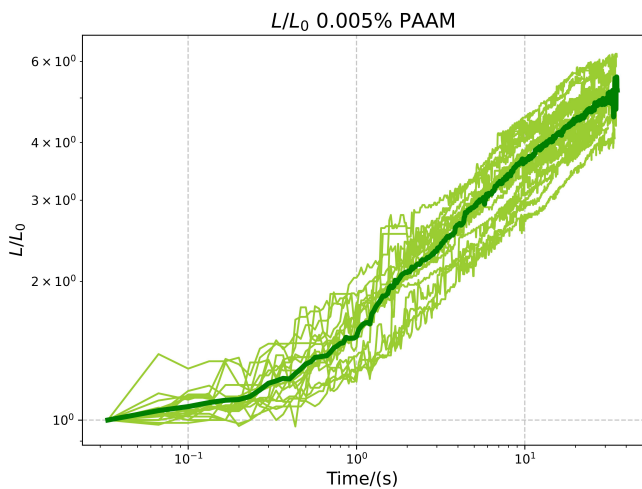


FIG. 13: Growth rate of the complex band for a concentration of 0.005% PAAM in log-log. In light green, the value of each experiment; in dark green, the mean value of all of them.

We have the same situation as before, at the beginning, the band grows more slowly, following a power law afterwards. The fact that there are two different velocities might mean that the phenomena governing each regime may differ. One possible explanation that can be given is that, before expanding, the colloid clusters collapse on themselves, nonetheless, further research should be conducted to find the origin of this difference.

3. Comparison

In Fig. 14, we can see the difference between the growth paces of both concentrations.

Here we can see that, for the higher concentration, the speed is greater, and I show in Fig. 15 the same graph in double-logarithmic plot. Since we do not have enough data to study the first region, in which the chain grows more slowly, we shall focus only on the second region, where there is a dependence of the type $\frac{L}{L_0} \propto t^\beta$. In this region, the exponent of the higher concentration seems to be larger than that measured from the experiments with smaller concentration of PAAM. In order to further examine this difference, let us perform a non-linear regression to the logarithm of this region of our data, and compare both slopes and intercepts, considering the dependence of L with t to be given by Eq. 7. In Fig. 16, we can see this fit.

$$\frac{L}{L_0} = \alpha t^\beta \quad (7)$$

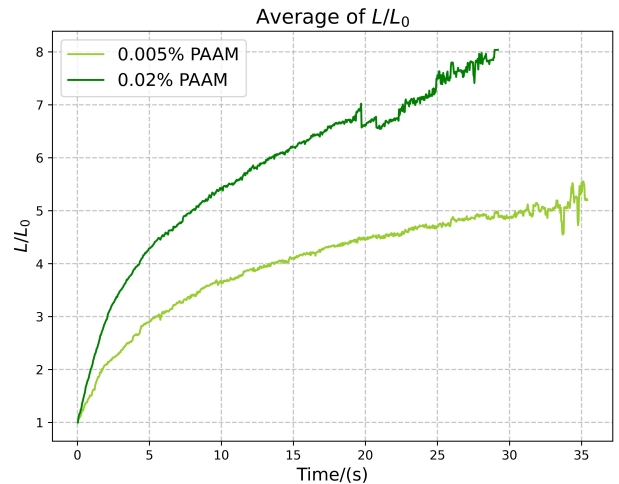


FIG. 14: Comparison between both growth rates.

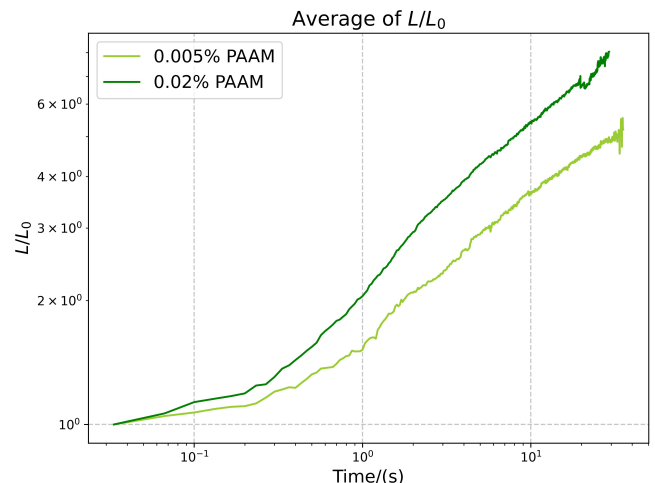


FIG. 15: Comparison between both growth rates in log-log.

Now the dependence is more obvious. In our fit, the exponent β for the 0.02% PAAM, solution is given by the slope, and it is $\beta = 0.362 \pm 0.052$, and the value of α , is given by the exponential of the intercept, which should have units of $t^{-\beta}$, and it is $\alpha = 2.351 \pm 0.309 s^{-\beta}$. On the other hand, for the other solution, $\beta = 0.319 \pm 0.033$ and $\alpha = 1.727 \pm 0.261 s^{-\beta}$. So, it may seem that both parameters have a dependence on the concentration of PAAM in water, and, the more highly concentrated the sample is, the faster the chain will grow.

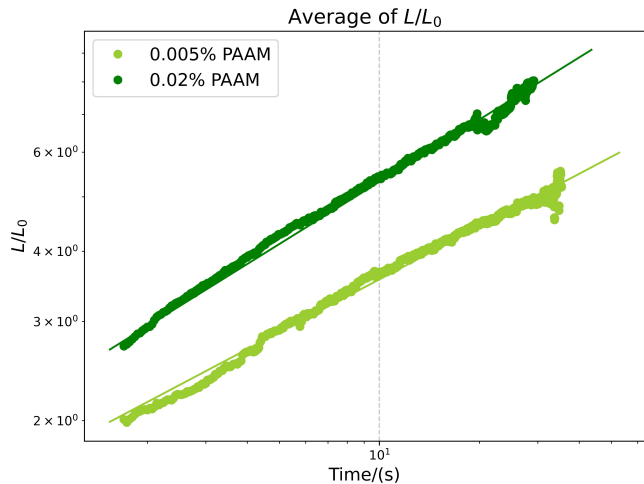


FIG. 16: Fits performed for the growth rate data.

B. Microscopical flow

To be able to understand this band formation phenomenon, it would be useful to observe how the flow around the magnetic colloids is, so as to have a better understanding on why particles choose to follow those patterns. In Figs. 17 & 18, we can see the flow for PAAM solutions of 0% and 0.05% respectively, obtained from a previous work by Gaspard, J. et al. [18]. It is convenient

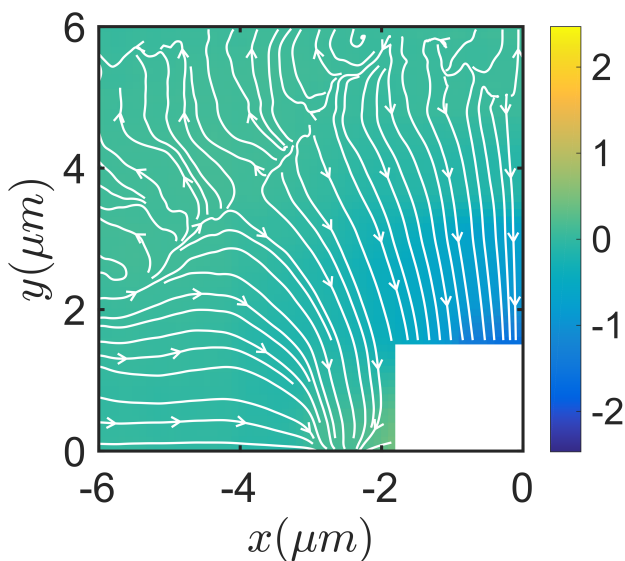


FIG. 17: Microscopic flow around the colloid at a concentration of 0% PAAM [18]. The units of the color bar are $\mu\text{m}/\text{s}$. Colors corresponding to positive values mean the flow is repulsive with respect to the colloid, whereas colors corresponding to negative values indicate an attractive flow with respect to the colloid.

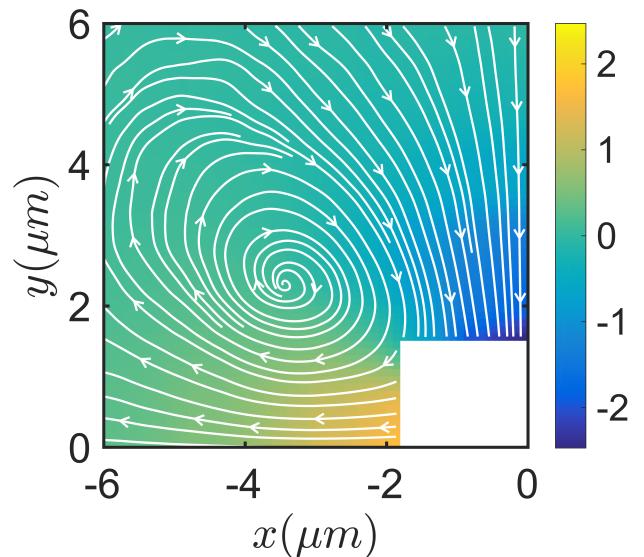


FIG. 18: Microscopic flow around the colloid at a concentration of 0.05% PAAM [18]. The units of the color bar are $\mu\text{m}/\text{s}$. Colors corresponding to positive values mean the flow is repulsive with respect to the colloid, whereas colors corresponding to negative values indicate an attractive flow with respect to the colloid.

to remember that the flow is symmetric with respect to the y and the x axis. It seems that, for both concentrations, there is a repulsive flow on the side of the magnetic colloid, whereas there is an attractive one on top of it. As can be seen, both the repulsive and the attractive flow's intensity increases with the PAAM concentration, with this former one being, in both cases, noticeably weaker than the latter one. The repulsive flow's strength seems to diminish faster than the attractive one. In both cases, there is a minimum: for the 0% PAAM concentration, this minimum is in line with the colloid, in the x axis, at around $2.5 \mu\text{m}$ of distance from the colloid, while the one for the 0.05% PAAM concentration forms an angle of a bit over 0.5 rad with respect to the horizontal. The situations seen for these two previous concentrations are quite different. There is a need to observe the evolution of the flow in between them. The context of this TFM project is to measure and analyse the flow of PAAM solutions with concentrations 0.02% and 0.005%, which are in between these values, to cover this existing gap. In Fig.19, we can see the microscopic flow for the 0.02% PAAM concentration.

As can be seen, we have a similar situation as in the case of 0.05% PAAM, however, both the attractive and repulsive forces are weaker. Additionally, the minimum value seems to be located on the coordinates $(-4, 47, 2.86)$, exactly on top of the spiral, at an angle $\theta = 0.5696 \text{ rad}$, which is roughly the same angle as for the 0.05% PAAM concentration, however, it seems to be further from the magnetic colloid, being at a distance of $5.311 \mu\text{m}$. This point might seem as a stagnation point, where

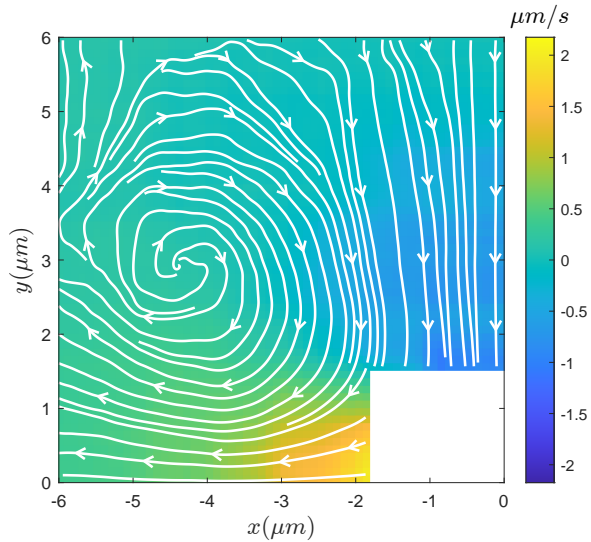


FIG. 19: Microscopic flow around the colloid at a concentration of 0.02% PAAM. Colors corresponding to positive values mean the flow is repulsive with respect to the colloid, whereas colors corresponding to negative values indicate an attractive flow with respect to the colloid.

flow velocity vanishes. Therefore, this point might be a center, and the spiral lines represent closed orbits around the center.

As for the 0.005% PAAM concentration, the microscopic flow can be seen in Fig. 20.

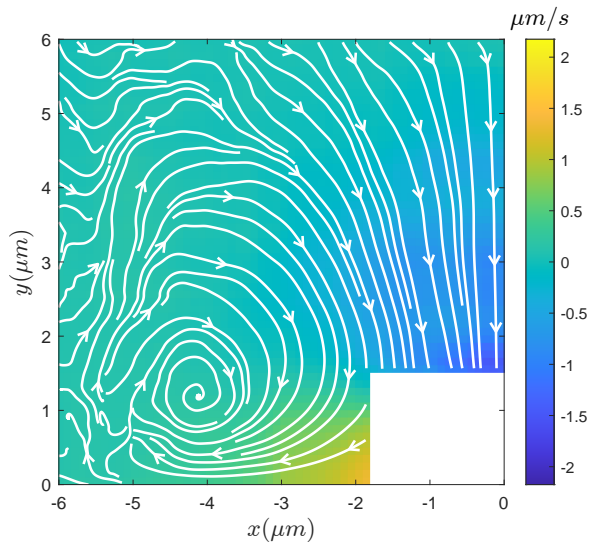
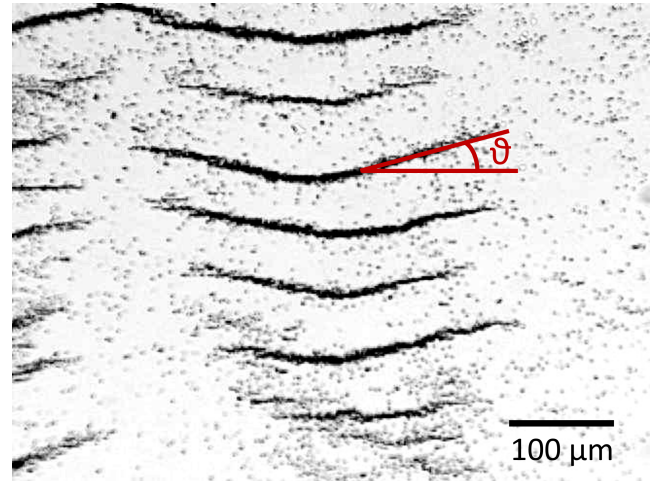
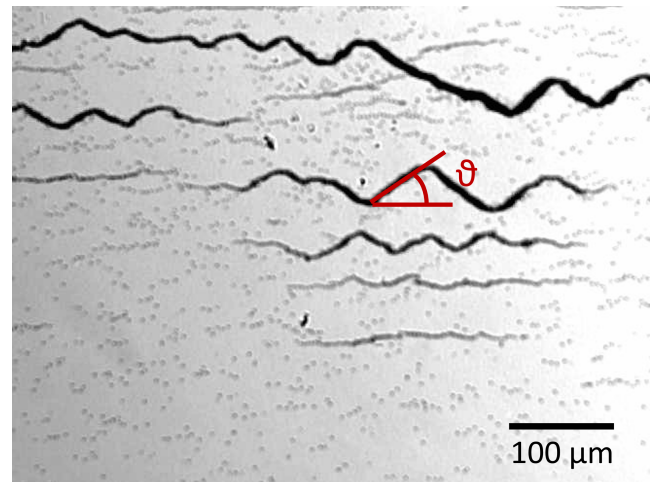


FIG. 20: Microscopic flow around the colloid at a concentration of 0.005% PAAM. Colors corresponding to positive values mean the flow is repulsive with respect to the colloid, whereas colors corresponding to negative values indicate an attractive flow with respect to the colloid.

As we can see, the flow’s strength has diminished, both its intensity and its range, which explains why the process of formation of the chain was also slower than in the previous case. Additionally, it presents a significantly greater decrease on the side of the colloid than on the top; as a result, the point of minimum flow is now closer to the horizontal line, specifically, on the coordinates $(-4.171, 1.156)$, at an angle of $\theta = 0.2703 \text{ rad}$ and a distance of $4.328 \mu\text{m}$ with respect to the center of the particle. This angle decrease is in good agreement with what was seen on the growth rate experiments, since the angle presented by the chains in the less concentrated solution was smaller, as can be seen in Fig. 21.



(a)



(b)

FIG. 21: Comparison between the angles of the zig-zag shaped chains at a concentration of (a) 0.005% and (b) 0.02% PAAM.

The angle seen in Fig. 21a is visibly higher than what expected from previous measurements. The reason for that, is because, as explained previously, the magnetic field applied does have a net component perpendicular to

the growing chain which may cause an effective attraction towards one direction. This attraction generates motion, and, the greater the density of colloids, the faster they move, as seen in the experiment undertaken by Gaspard, J. et al. [10], i.e., the center of the band, which has a larger number of colloids, will move faster towards this direction than the sides, causing the chain to bend. This effect is negligible for the 0.02% PAAM solution, since the elastic forces of the fluid that oppose this motion are larger, however, it can be seen for the 0.005% PAAM solution.

In Figs. 23 & 22, we can see the microscopic flows for the 0.005% and 0.02% PAAM concentration but in polar coordinates. As can be observed, both the attractive

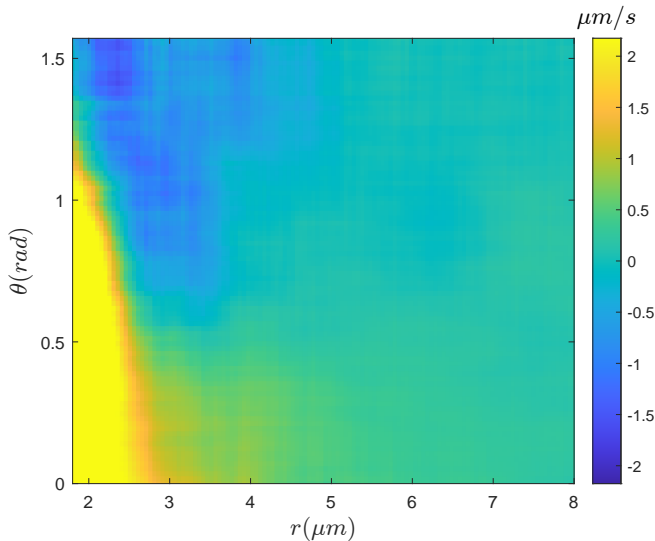


FIG. 22: Microscopic flow around the colloid at a concentration of 0.02% PAAM in polar coordinates. Colors corresponding to positive values mean the flow is repulsive with respect to the colloid, whereas colors corresponding to negative values indicate an attractive flow with respect to the colloid.

and the repulsive flows have a further reach and a higher intensity in the more concentrated solution.

From this analysis, we can see that the larger the concentration of PAAM, the stronger the hydrodynamic forces are, with the repulsive component increasing faster than the attractive one. Also, we see how the position of the minimum rises in the y axis from the 0% PAAM solution until the 0.02% PAAM concentration, however, from the 0.02% PAAM concentration until the 0.05% PAAM solution, it stops rising, and starts approaching the colloid.

V. CONCLUSIONS AND FUTURE WORK

From the first part of this TFM related with the growth rate of the chain, we can conclude that the length of the

chain as a function of time does seem to fit a power law,

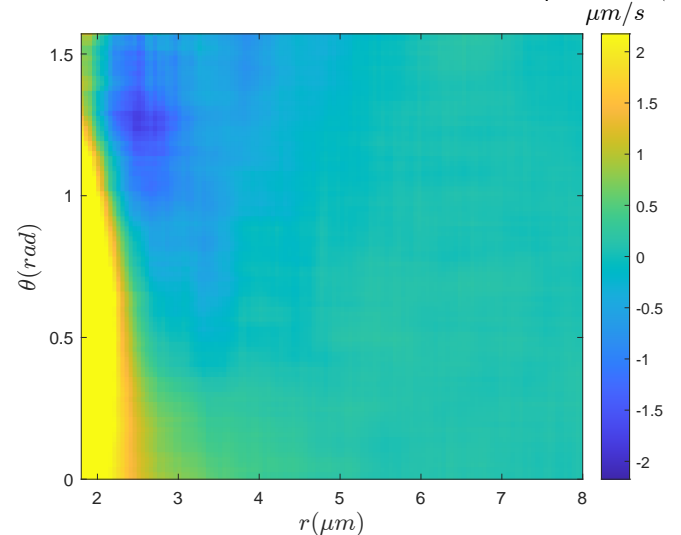


FIG. 23: Microscopic flow around the colloid at a concentration of 0.005% PAAM in polar coordinates. Colors corresponding to positive values mean the flow is repulsive with respect to the colloid, whereas colors corresponding to negative values indicate an attractive flow with respect to the colloid.

in which the exponent depends on the PAAM concentration. Moreover, the more concentrated the solution is, the faster the chain grows. I have analyzed the chain growth for different polymer concentration in water, spanning from 0% to 0.02%. However, longer measurements should be done, to better determine the exponents of the power law and the chain growth dynamics. Also, the initial region of the formation of the band seems to follow a different growth law, it would be interesting to further study this regime. Additionally, the dependence of the growth speed and the value of the concentration of PAAM should be addressed.

From the microscopic flow experiment we see that non-magnetic particles feel this attraction towards the shaking colloid, and in an apparently similar way to the attraction felt by magnetic ones, meaning hydrodynamic effects play a major role with respect to magnetic ones. Also, we see that the angle at which the equilibrium position of the hydrodynamic flow, which conditions the shape of the chains, depends as well on the concentration of PAAM, more measurements should be done to find this dependence. At around 0.02%, the value of this angle seems to saturate, with the equilibrium point seemingly approaching the colloid with the increasing concentration, it would be interesting to find what happens if we keep increasing the PAAM concentration.

- [1] Gomez-Solano, J. R., Blokhuis, A., & Bechinger, C. (2016). *Dynamics of self-propelled Janus particles in viscoelastic fluids*. Physical review letters, 116(13), 138301.
- [2] Tung, C. K., Lin, C., Harvey, B., Fiore, A. G., Ardon, F., Wu, M., & Suarez, S. S. (2017). *Fluid viscoelasticity promotes collective swimming of sperm*. Scientific reports, 7(1), 3152.
- [3] Lozano, C., Gomez-Solano, J. R., & Bechinger, C. (2019). *Active particles sense micromechanical properties of glasses*. Nature Materials, 18(10), 1118-1123.
- [4] Gaojin, L., Eric, L., & Ardekani, A. M. (2021). *Microswimming in viscoelastic fluids*. JOURNAL OF NON-NEWTONIAN FLUID MECHANICS, 297.
- [5] Baraban, L., Harazim, S. M., Sanchez, S., & Schmidt, O. G. (2013). *Chemotactic behavior of catalytic motors in microfluidic channels*. Angewandte Chemie, 125(21), 5662-5666.
- [6] D'Avino, G., & Maffettone, P. L. (2015). *Particle dynamics in viscoelastic liquids*. Journal of Non-Newtonian Fluid Mechanics, 215, 80-104.
- [7] Puente-Velázquez, J. A., Godínez, F. A., Lauga, E., & Zenit, R. (2019). *Viscoelastic propulsion of a rotating dumbbell*. Microfluidics and Nanofluidics, 23, 1-7.
- [8] Aranson, I. S. (2013). *Active colloids*. Physics-Uspekhi, 56(1), 79.
- [9] Martínez-Pedrero, F., Navarro-Argemí, E., Ortiz-Ambriz, A., Pagonabarraga, I., & Tierno, P. (2018). *Emergent hydrodynamic bound states between magnetically powered micropropellers*. Science advances, 4(1), eaap9379.
- [10] Junot, G., Cebers, A., & Tierno, P. (2021). *Collective hydrodynamic transport of magnetic microrollers*. Soft Matter, 17(38), 8605-8611.
- [11] Ghannam, M. T., & Esmail, M. N. (1998). *Rheological properties of aqueous polyacrylamide solutions*. Journal of applied polymer science, 69(8), 1587-1597.
- [12] Pusey, P. N. (1991). *Liquids, freezing and the glass transition*. Les Houches Summer Schools of Theoretical Physics Session LI (1989).
- [13] Mason, T. G. (2000). *Estimating the viscoelastic moduli of complex fluids using the generalized Stokes-Einstein equation*. Rheologica acta, 39(4), 371-378.
- [14] Sanematsu, P. C., Erdemci-Tandogan, G., Patel, H., Retzlaff, E. M., Amack, J. D., & Manning, M. L. (2021). *3D viscoelastic drag forces contribute to cell shape changes during organogenesis in the zebrafish embryo*. Cells & Development, 168, 203718.
- [15] A. M. Purcell. *Life at Low Reynolds Number*. American Journal of Physics 45, 3-11 (1977).
- [16] Happel, J., & Brenner, H. (1973). *Low reynolds number hydrodynamics*. Noordhoff int. Publishing, Leyden, Netherland, 235.
- [17] Tierno, P., Muruganathan, R., & Fischer, T. M. (2007). *Viscoelasticity of dynamically self-assembled paramagnetic colloidal clusters*. Physical review letters, 98(2), 028301.
- [18] Gaspard, J., Corato, M., & Tierno, P. (2023). *Large scale zig-zag pattern emerging from circulating active shakers*. PRE PRINT.